Scripta Materialia 123 (2016) 118–121

Contents lists available at ScienceDirect

Scripta Materialia

journal homepage: www.elsevier.com/locate/scriptamat

Regular Article

Understanding the spark plasma sintering from the view of materials joining

Peng Dong [a,b,*], Zhe Wang [a,c], Wenxian Wang [a,b], Shaoping Chen [a], Jun Zhou [d]

[a] College of Materials Science and Engineering, Taiyuan University of Technology, Taiyuan 030024, China
[b] Shanxi Key Laboratory of Advanced Magnesium-based Materials, Taiyuan 030024, China
[c] College of Materials Science and Engineering, Harbin Institute of Technology, Harbin 150001, China
[d] Department of Mechanical Engineering, Pennsylvania State University Erie, Erie, PA 16563, USA

ARTICLE INFO

Article history:
Received 20 May 2016
Received in revised form 14 June 2016
Accepted 14 June 2016
Available online xxxx

Keywords:
Spark plasma sintering
Mechanism
Interface
Materials joining

ABSTRACT

Spark plasma sintering (SPS) is an attractive consolidation process. However, the mechanism behind this process is still an open topic for debate. This paper presents the first attempt to understand the SPS mechanism from perspective of materials joining. For this, $TiNi_f$/Al composites were fabricated by SPS, and the interfacial microstructures were investigated using field emission scanning electron microscopy and transmission electron microscopy. According to the experimental results, several joining processes were reflected well during SPS, involving micro-arc welding, electric resistance welding and diffusion welding. The proposed understanding of SPS will be helpful to the control of sintering quality.

Spark plasma sintering (SPS) is an attractive consolidation process which offers the possibility of fabricating highly densified bulk materials within a short time and low sintering temperature [1]. SPS has been used effectively for the densification of various materials from magnetic materials to thermoelectrics and even ceramics [2]. However, the mechanisms behind this process still remain unclear.

Originally, the most commonly accepted mechanism was that the high-energy pulse DC current induces the spark discharge and rapid Joule heating between the particles which result in the generation of plasma at high temperature, causing sintering [1,3,4]. This is how the name Spark Plasma Sintering was established. Unfortunately, the experimental evidences for the spark discharge and/or plasma are still very much lacking. In particular, Hulbert et al. [5] and Hitchcock et al. [6] successively gave an experimental demonstration of the absence of spark discharge and plasma either during the whole stage of SPS process. But recently, Zhang et al. [7] directly observed the occurrence of spark discharge during SPS, and the experimental results from Marder et al. [8] also strongly support the presence of spark and plasma during SPS.

The exact nature of the SPS mechanism is therefore still under debate. Santanach et al. [9] suggested the SPS showed two densification regimes: mechanisms including thermal-diffusion and local melting of grain surfaces at lower temperature, and volume diffusion at higher temperature. Song et al. [10] proposed a "self-adjusting" mechanism. Zhang et al. [11] described the sintering mechanisms as the sequence of the following stages: activation and refining of the powder, formation of the sintering neck, growth of the sintering neck and plastic deformation densification.

In essence, the SPS is a method that makes countless powder particles to become bulk material with the elimination of gaps and formation of metallurgical bonding among powder particles, which are the indispensable prerequisites of obtaining high-quality bulk materials. This is consistent with materials joining in nature with a main difference in scale. Actually, SPS was employed to join ceramics such as α-SiAlON [12], β-SiC [13], ZrB_2-SiC [14], C/SiC composites [15] and SiC-graphite [16] in last few years. However, more attentions were focused on the joining process (likewise the choice of fillers, the effect of pressure and dwell time, etc.) and the joint strength. The main objective of this paper is to understand the SPS from the perspective of materials joining, providing a new cognition for it.

Starting materials were spherical 2024Al (AlCu alloy) powders and Ti–50.2 at.% Ni fiber. $TiNi_f$/Al composites were fabricated by means of spark plasma sintering (Dr Sinter SPS-331LX, Fuji Electronic Industrial), as shown in Fig. 1. SPS has been carried out at 550 °C far below the melting temperature of 2024Al matrix ($T_m \approx 646$ °C) and TiNi fiber ($T_m \approx 1310$ °C), with a protection of Ar gas, applying different pressures (5 MPa, 50 MPa and 100 MPa) for 30 min.

After sintering, the samples were cut by using an electrical discharge cutting machine for microstructure examination and tensile tests, as illustrated in Fig. 1. Prior to microstructure examination all the samples were prepared by applying standard metallographic procedures. The

* Corresponding author at: College of Materials Science and Engineering, Taiyuan University of Technology, Taiyuan 030024, China.
E-mail address: dongpeng@tyut.edu.cn (P. Dong).

http://dx.doi.org/10.1016/j.scriptamat.2016.06.014
1359-6462/

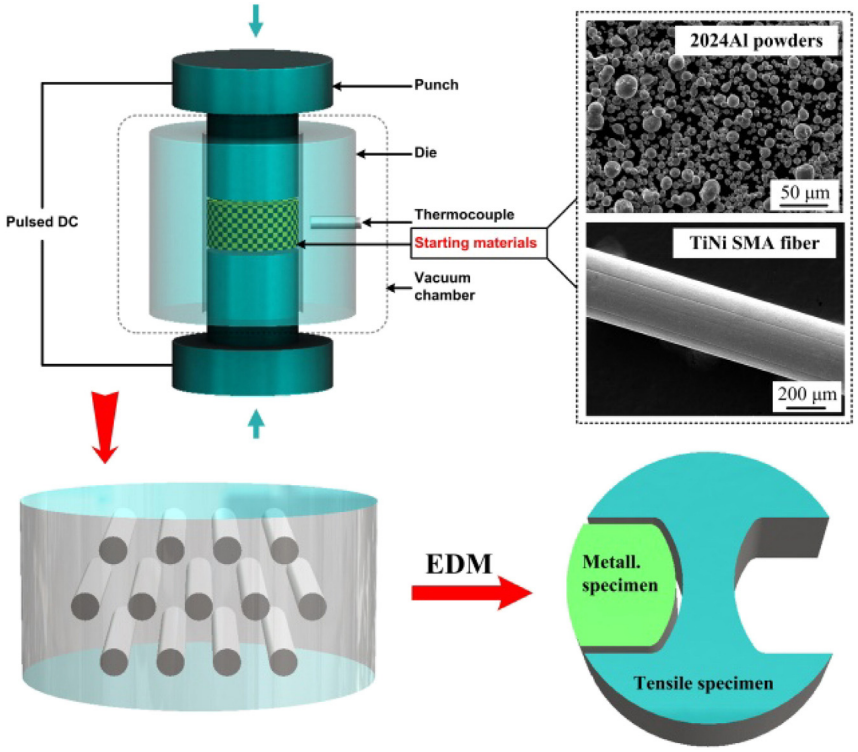

Fig. 1. Schematic for fabrication of $TiNi_f$/2024Al composites and preparation of specimens.

microstructure and fracture surfaces of the sintered $TiNi_f$/Al composites were investigated using a field emission scanning electron microscopy (FESEM; TESCAN MIRA3 LM) equipped with EDS system. Moreover, the interfacial microstructure between $TiNi_f$ and Al matrix was investigated by a high-resolution transmission electron microscopy (HRTEM; JEOL 2100F) at an acceleration voltage of 200 kV. And the TEM foil samples were prepared at a SEM/FIB crossbeam workstation (TESCAN LYRA3).

Fig. 2a presents the typical SEM images of the $TiNi_f$/Al composite fabricated with 50 MPa pressure. It is apparent that a relatively uniform interface layer between matrix and fibers were formed. The composite fabrication can be ragarded as multi-materials joining involving the joining of Al particles and the joining between Al particles and TiNi fibers. In this case, the interface layers are the heterogeneous welds while the homogeneous welds of Al particles are seamless due to the nearly full dense composite. Thus, soundly metallurgical bonding was achieved within Al-Al and Al-$TiNi_f$.

High magnification image taken from a heterogeneous weld shows that it consists of alternating phases, resulting in a quasi-lamellar morphology, as shown in Fig. 2b. This phenomenon can be attributed the effects of electric field which enhances the diffusivity, thus promoting migration of ions through the joining interface. Further, EDS analysis was carried out and the results were inserted in Fig. 2b. The chemical composition changes across the weld indicate that the grey white phases are rich in Al and Ni while the grey dark phases are rich in Al and Ti. And the atomic ratio of the grey white phases (marked as W) and grey dark phases (marked as D) are Al/Ni ≈ 3 and Al/Ti ≈ 3, respectively.

Fig. 3a shows the TEM bright and dark field image at low magnification of the heterogeneous weld, further validating it contains double phases. Fig. 3b gives the corresponding selected area electron-diffraction pattern, showing heterogeneous weld was the mixture of Al_3Ti and Al_3Ni phases.

Tensile tests for sintered composites were conducted to investigate the joining state of homogeneous welds between 2024Al particles. Fig. 4a shows the micrograph of fracture surface taken from the Al matrix within the composites sintered at 50 MPa pressure, the 2024Al matrix exhibits typical ductile dimple facture pattern without discernibility of starting Al powders. This indicates that the strong joining between Al particles was obtained, giving the strength of homogeneous welds compares favourably with that of base Al.

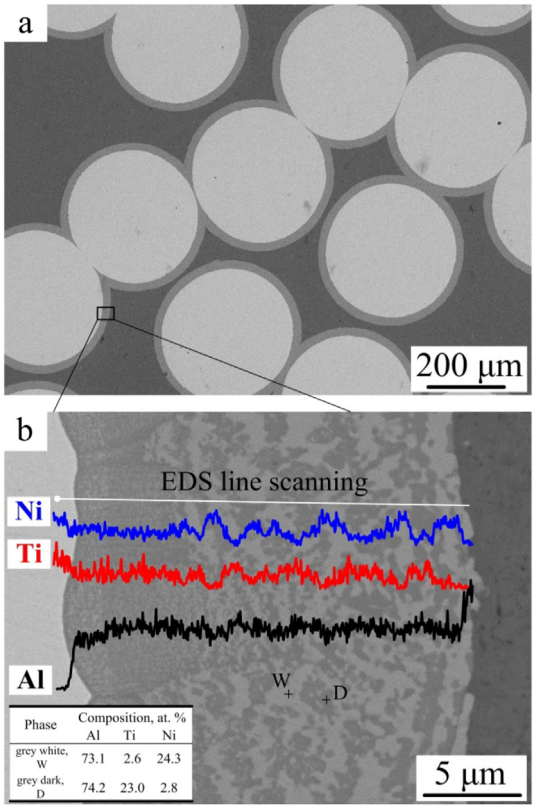

Fig. 2. The typical SEM BSE images of $TiNi_f$/Al composite at low magnification (a) and high magnification (b) inserted with EDS results.